Available online at www.sciencedirect.com
SCIENCE DIRECT®
ELSEVIER
Journal of Sound and Vibration 290 (2006) 369–387
JOURNAL OF SOUND AND VIBRATION
www.elsevier.com/locate/jsvi

Damage detection by finite element model updating using modal flexibility residual

Bijaya Jaishi[a], Wei-Xin Ren[a,b,*]

[a]Department of Civil Engineering, Fuzhou University, Fuzhou, Fujian Province 350002, PR China
[b]Department of Civil Engineering, Central South University, Changsha, Hunan Province 410075, PR China

Received 25 May 2004; received in revised form 15 November 2004; accepted 2 April 2005
Available online 22 June 2005

Abstract

A sensitivity-based finite element (FE) model updating is carried out for damage detection in this paper. The objective function consisting of the modal flexibility residual is formulated and its gradient is derived. The optimization algorithm used to minimize the objective function and damage detection procedures are explained. The proposed procedure is firstly illustrated with a simulated example of the simply supported beam. The effect of noise on the updating algorithm is studied. It is demonstrated that the behavior of proposed algorithm on noise is satisfactory and the identified damage patterns are good. Afterwards, the procedure is applied for the tested reinforced concrete beam, which is damaged in the laboratory. Despite all the elements in the FE model are used as updating parameters which is considered as the extreme adverse condition in FE model updating, the identified damage pattern is comparable with those obtained from the tests. It is verified that the modal flexibility is sensitive to damage and the proposed procedure of FE updating using the modal flexibility residual is promising for the detection of damaged elements.

1. Introduction

Quantitative and objective condition assessment for infrastructure protection has been a subject of strong research within the engineering community. To achieve this aim, methodologies

*Corresponding author. Tel.: +86 591 7892454; fax: +86 591 3737442.
E-mail address: ren@fzu.edu.cn (W.-X. Ren).
URL: http://bridge.fzu.edu.cn.

0022-460X/$ - see front matter
doi:10.1016/j.jsv.2005.04.006

of the routine inspections with fixed intervals or the continuous monitoring, which provide constant information on safety reliability or remaining lifetime of the structure, have been under development in recent years. Inspection of structural components for damage is vital to take decisions about their repair or retirement. Visual inspection is tedious and often does not yield a quantifiable result [1]. For some components visual inspection is virtually impossible. Methods which are based on pure signal processing have only a limited capability for the early detection of damage and often do not allow unique conclusions to be drawn on the sources of the damage [2]. The importance and difficulty of the damage detection problem has caused a great deal of research on the quantitative methods of damage detection based upon physical testing. Among those physical tests, the use of the modal tests has emerged as an effective tool to use in damage detection. The possibility of using measured vibration data to detect changes in structural systems due to damage has gained increasing attention [3,4]. Doebling et al. [5] gave a detail overview of the vibration based damage detection methods.

Many modal-based damage detection methods attempt to detect changes in the natural frequencies of a structure. In an earlier work by Cawley and Adams [6], it was shown that the ratio of frequency changes in different modes is only a function of damage location and not the magnitude of damage. Salawu [7] reviewed the different methods of structural damage detection through changes in natural frequencies. He emphasized the simplicity and low cost of this approach, but at the same time pointed out the factors that could limit successful application of vibration monitoring to damage detection and structural assessment since the changes in natural frequencies cannot provide the spatial information about structural damage. Therefore, also mode shape information is needed to uniquely localize the damage. Analysis of changes in mode shapes due to damage represents another subgroup of modal-based methods. Usually, changes in a mode shape's curvature are more sensitive to damage. Pandey et al. [8] introduced the use of mode shape curvatures. Changes in strain energy were used as an indicator to represent damage [9]. In fact, the mode shape curvature is correspondent to the strain energy at that location.

Another class of damage identification methods uses the dynamically measured modal flexibility matrix. Aktan et al. [10] proposed the use of the measured flexibility as a "condition index" to indicate the relative integrity of a bridge. Two bridges were tested and the measured flexibility was compared to the static deflections induced by a set of truck-load tests. Pandey and Biswas [11] presented a damage detection and location method based on changes in the measured modal flexibility of the structure. This method is applied to several numerical examples and to an actual spliced beam where the damage is linear in nature. Results of the numerical and experimental examples showed that estimates of the damage condition and the location of the damage could be obtained from just the first two measured modes of the structure. It is demonstrated that the modal flexibility is more sensitive to damage than the natural frequency or mode shape. Reisch and Park [12] proposed a method of structural health monitoring based on relative changes in localized flexibility properties and applied for the damage detection of elevated highway bridge column. Topole [13] developed an algorithm to calculate the contribution of the flexibility of the structural members to the sensitivity of the modal parameters to change on the flexibilities of the members and applied to detect the damage of simulated structure with truss member.

Finite element (FE) model updating can be one of the other ways to identify the structural damage and perform the assessment of the structure. The purpose of FE model updating is to modify the mass, stiffness and damping parameters of the numerical model in order to obtain better agreement between numerical results and test data. A number of model updating methods in structural dynamics have been proposed [14–17]. Non-iterative methods directly update the elements of stiffness and mass matrices are one-step procedures [18,19]. The resulting updated matrices reproduce the measured structural modal properties exactly but do not generally maintain structural connectivity and the corrections suggested are not always physically meaningful. The iterative parameter updating method involves using the sensitivity of the parameters to find their changes [15,17]. This sensitivity-based parameter updating approach has an advantage of identifying parameters that can directly affect the dynamic characteristics of the structure. Fritzen et al. [2] examined the problem of detecting the location and extent of structural damage from measured vibration test data using FE model updating. It is noted that the mathematical model used in the model updating is usually ill-posed and the special attention is required for an accurate solution. Wang et al. [20] implemented FE model updating to establish the baseline modal values (modal frequencies and mode shapes) for a long-span bridge. They suggested that model updating might be used in automated on-line monitoring on bridges. In recent years, sensitivity-based FE model updating has been successfully used for damage assessment of structures [21,22].

Selection of the residuals in the objective function is a crucial issue in FE model updating. It not only affects the interpretation of the best correlation, but also influences the behavior of the utilized optimization algorithm. The objective function is normally built up by the residuals between the measurement results and the numerical predictions. Frequency residual and modal accuracy criterion (MAC)-related function were used in FE model updating of industrial structures [23]. The residual vector containing the deviation from the orthogonality of the experimental mode shapes to the analytical ones was discussed in literature [24]. Some of the sensitivity-based approaches reported for FE model updating of real case studies have considered only the frequencies as the backbone during optimization [22,25]. FE model updating method was successfully applied to the damage assessment of structures using frequency and mode shape residual with the introduction of damage functions [26,27]. For the purpose of damage detection, the residuals should be sensitive to even slight local structural changes. The modal flexibility is basically a combination of natural frequencies and mode shapes, which is a sensitive index in damage detection, so the modal flexibility residual in the objective function is used.

In this paper, a sensitivity-based FE model updating is carried out for the purpose of damage detection. The objective function consisting of the modal flexibility residual is formulated and its gradient is derived. The optimization algorithm used to minimize the objective function and damage detection procedures are presented. The proposed procedure is illustrated with simulated beam and the laboratory-tested beam with damage. Despite all the elements in the FE model are used as updating parameters, which is considered as the extreme adverse condition in FE model updating, the identified damage pattern is comparable. It is demonstrated that the proposed FE updating using the modal flexibility residual is promising for the detection of damaged elements.

2. Theoretical background

2.1. Objective functions and minimization problem

The undamped free vibration of a structural dynamic system can be described by the second-order differential equation as

$$[M]\{\ddot{u}\} + [K]\{u\} = 0 \tag{1}$$

in which $[M]$ and $[K]$ are the mass and stiffness matrices, respectively, and u is the displacement vector. The eigensolution of this system consists of the eigenvalue matrix $[\Lambda]$, which is a diagonal matrix of the squared natural frequencies, diag$\{\omega_i^2\}$, and the eigenvector matrix $[\phi]$, which is mass-normalized, i.e. scaled such that

$$[\phi]^{\mathrm{T}}[K][\phi] = [\Lambda], \tag{2}$$

$$[\phi]^{\mathrm{T}}[M][\phi] = [I]. \tag{3}$$

Solving Eq. (2), the stiffness matrix can be written in modal form as

$$[K] = [\phi]^{-\mathrm{T}}[\Lambda][\phi]^{-1} = ([\phi][\Lambda]^{-1}[\phi]^{\mathrm{T}})^{-1}. \tag{4}$$

The flexibility is basically defined as the inverse of the stiffness matrix

$$[G] \equiv [K]^{-1}. \tag{5}$$

Substituting Eq. (4) into Eq. (5) yields the inverse vibration representation of the flexibility matrix

$$[G] \equiv [\phi][\Lambda]^{-1}[\phi]^{\mathrm{T}}. \tag{6}$$

If all the mode shapes and frequencies are available at all the DOFs, Eq. (6) gives the flexibility matrix and this flexibility matrix is exactly equal to the static flexibility matrix. The flexibility matrix can be separated into modal component and residual component. The contribution of the unmeasured vibration modes to flexibility is called the residual flexibility. The eigensolution used to form $[G]$ in Eq. (6) is the full eigensolution for the system. In practice, however, only a few lower mode shapes and frequencies are actually measured during vibration testing. Defining the measured modal set as n and unmeasured set as r the eigensolution can be partitioned as

$$[G] = [G_n] + [G_r], \tag{7}$$

where $[G_n]$ is the modal flexibility, formed from the measured modes and frequencies as

$$[G_n] = [\phi_n][\Lambda_n]^{-1}[\phi_n]^{\mathrm{T}} \tag{8}$$

and $[G_r]$ is the residual flexibility formed from the residual modes and frequencies as

$$[G_r] = [\phi_r][\Lambda_r]^{-1}[\phi_r]^{\mathrm{T}}. \tag{9}$$

In practice, the measured flexibility matrix is not computed for the full DOF set, because only a limited number of measurements are available. Partitioning the full DOF set into measured m and non-measured DOFs and multiplying the partitioned, it is shown in the work of

Doebling [28] that

$$[G_{mm}] = [\phi_{n_m}][\Lambda_n]^{-1}[\phi_{n_m}]^{\mathrm{T}} + [\phi_{r_m}][\Lambda_r]^{-1}[\phi_{r_m}]^{\mathrm{T}}, \tag{10}$$

where $[G_{mm}]$ is called the measured flexibility matrix; ϕ_{n_m} and ϕ_{r_m} are, respectively, the measured and unmeasured mode shapes of the structure at the measured DOFs; and Λ_n and Λ_r correspond to the eigenvalues of measured and unmeasured modes. The first and second portion of Eq. (10) indicate the modal and residual contribution to measured flexibility, respectively.

Doebling [28] developed a method to accurately estimate the static flexibility of the structure considering residual flexibility for forced vibration case in which the input of the system is known. For the case of known input, there is no problem to compute the residual flexibility. The issue considered in this work is related to the ambient vibration work, where the input of the system is not measured. For the case of unknown input with measurements carried out only in certain locations, the situation is much more different and the calculation of residual flexibility is not straightforward. In general, the measured modes are typically those that are lower in frequency and therefore contribute the most to the flexibility. Therefore, a good estimate of the flexibility matrix may be obtained from only a few low-frequency modes corresponding to measured DOFs [11,29–32]. Hence, Eq. (10) becomes

$$[G_{mm}] = [\phi_{n_m}][\Lambda_n]^{-1}[\phi_{n_m}]^{\mathrm{T}}. \tag{11}$$

For the sake of clarity, the measured flexibility matrix $[G_{mm}]$ will be referred to simply as $[G_{\mathrm{exp}}]$, Φ_{n_m} will be referred as ϕ and Λ_n will be referred as Λ in the remaining portion of the paper. Similarly, the notation for matrix [ ] is removed for convenience.

Eq. (11) is used to compute the modal flexibility and used for the model updating procedure in the paper. The analytical modal flexibility is estimated using the analytical eignevalue and mode shapes which are partitioned corresponding to the measured DOFs. The most important issue to use Eq. (11) is the mass normalization of mode shapes obtained from ambient vibration test. In general, there are three methods to mass normalize the ambient vibration mode shapes. They are the FE model approach [30], sensitivity-based method [33], and the methods that use mass orthogonality condition [34]. In case of FE model updating application, the first approach of using the FE mass matrix to normalize the experimental mode shape is straightforward due to the fact that the detail analytical model of the complex structure is readily available.

An objective function Π reflects the deviation between the analytical prediction and the real behavior of a structure. The FE model updating can be posed as a minimization problem to find x^* design set such that

$$\Pi(x^*) \leqslant \Pi(x), \quad \forall x, \tag{12}$$

$$x_{li} \leqslant x_i \leqslant x_{ui}, \quad i = 1, 2, 3, \ldots n,$$

where the upper and lower bounds on the design variables are required. The general objective function is formulated in terms of the discrepancy between FE and experimental quantities. The modal flexibility error residual is given by the expression

$$G(X) = G_{\mathrm{exp}} - G_{\mathrm{ana}} \tag{13}$$

in which G_{exp} is the measured modal flexibility matrix obtained at the measurement DOF; G_{ana} is the analytical flexibility matrix corresponding to the measured DOF; and X is the updating parameters which is a column matrix. The updating parameters are the uncertain physical properties of the numerical model. Instead of the absolute value of each uncertain variable X, its relative variation to the initial value X_0 is chosen as dimensionless updating parameter a. Using the normalized parameters a, problems of numerical ill-conditioning due to large relative differences in parameter magnitudes can be avoided:

$$a^i = -\frac{X^i - X_0^i}{X_0^i}, \tag{14a}$$

$$X^i = X_0^i(1 - a^i). \tag{14b}$$

The objective of FE model updating problem is to find the value of vector a^i of Eq. (14) which minimizes the error between the measured and analytical modal flexibility matrices. Hence, Eq. (13) becomes

$$\min_a \|G(a)\|, \tag{15}$$

where

$$G(a) = G_{\exp} - \phi \Lambda^{-1} \phi^{\mathrm{T}}. \tag{16}$$

In Eq. (16), ϕ indicates the analytical mode shape matrix corresponding to the experimental degree of freedom and Λ denotes the frequency matrix containing the square of circular natural frequency. Eq. (15) represents the function to be minimized, which is obviously in matrix form. To carry out the minimization of matrix in least square sense, the norm of matrix called Frobenius Norm is utilized in this work. Hence, the minimization problem using Frobenius Norm can be presented as

$$\min_a \|G(a)\|_F^2. \tag{17}$$

The most frequently used matrix norms is the F-norm (Frobenius norm). The F-norm is used to provide the least-square solution of an exact or over-determined system of equations. It is a norm of $m \times m$ matrix A defined as the square root of the absolute square sum of its elements. Mathematically, for $[A] \in \mathbb{R}^{m\times m}$

$$\|A\|_F = \sqrt{\sum_{j=1}^{m}\sum_{k=1}^{m} |a_{jk}|^2}. \tag{18}$$

Hence, substituting Eq. (18) into Eq. (17), the function to be minimized becomes

$$\|G(a)\|_F^2 = \sum_{j=1}^{m}\sum_{k=1}^{m} (G_{jk}(a))^2. \tag{19}$$

To avoid the numerical problems during minimization, this function is divided by the function value at the initial parameter estimate:

$$\Pi(a) = \frac{\|G(a)\|_F^2}{\|G(a_0)\|_F^2}. \tag{20a}$$

As a result, finally, the minimization problem can be mathematically posed as

$$\begin{aligned} &\min_{a} \quad \Pi(a) \\ &\text{such that } a_{li} \leqslant a_i \leqslant a_{ui}, \quad i = 1, 2, 3, \ldots, N. \end{aligned} \tag{20b}$$

2.2. Objective function gradient

The Trust Region Newton algorithm as implemented in the Optimization Toolbox of MATLAB [35] is used to solve the minimization problem of Eq. (20b). To this end, the objective function gradient is needed. The gradient is found by taking the derivatives of Π in Eq. (20a) with respect to a_i

$$\frac{\partial \Pi}{\partial a_i} = \frac{1}{\left\| G(a_0) \right\|_F^2} \sum_{j=1}^{m} \sum_{k=1}^{m} 2 G_{jk}(a) \left(\frac{\partial}{\partial a_i} G(a) \right)_{jk}, \tag{21}$$

where $(\partial/\partial a_i)\, G(a)$ is calculated by taking the partial derivative of Eq. (16) with respect to a_i, which is shown below:

$$\begin{aligned} \frac{\partial G}{\partial a_i} &= -\frac{\partial}{\partial a_i} (\phi \Lambda^{-1} \phi^{\mathrm{T}}), \\ \frac{\partial G}{\partial a_i} &= -\left[\frac{\partial \phi}{\partial a_i} (\Lambda^{-1} \phi^{\mathrm{T}}) + \phi \frac{\partial}{\partial a_i} (\Lambda^{-1} \phi^{\mathrm{T}}) \right], \end{aligned} \tag{22a}$$

$$\frac{\partial G}{\partial a_i} = -\left[\frac{\partial \phi}{\partial a_i} (\Lambda^{-1} \phi^{\mathrm{T}}) + \phi \frac{\partial \Lambda^{-1}}{\partial a_i} (\phi^{\mathrm{T}}) + \phi \Lambda^{-1} \frac{\partial}{\partial a_i} (\phi^{\mathrm{T}}) \right]. \tag{22b}$$

In matrix algebra, it is shown that the partial derivative of the inverse of a matrix may be written as

$$\frac{\partial \Lambda^{-1}}{\partial a_i} = -\Lambda^{-1} \frac{\partial \Lambda}{\partial a_i} \Lambda^{-1}. \tag{23}$$

Hence, substituting Eq. (23) into Eq. (22b) yields

$$\frac{\partial G}{\partial a_i} = -\left[\frac{\partial \phi}{\partial a_i} (\Lambda^{-1} \phi^{\mathrm{T}}) - \phi \Lambda^{-1} \frac{\partial \Lambda}{\partial a_i} \Lambda^{-1} \phi^{\mathrm{T}} + \phi \Lambda^{-1} \frac{\partial}{\partial a_i} (\phi^{\mathrm{T}}) \right]. \tag{24}$$

From Eq. (24), it is recognized that the derivatives of FE eigenvalues and eigenvectors have to be evaluated to calculate the objective function gradient.

2.3. Eigenpair derivatives

The calculation of eigenvalue and eigenvector derivatives has been extensively studied and reported in many papers. In this study, the expressions derived by Fox and Kapoor [36] are used. Differentiating the generalized eigenvalue problem with respect to the design variables and using the orthogonalization properties of eigenvectors, one arrives at

$$\frac{\partial \lambda_j}{\partial a_i} = \phi_j^{\mathrm{T}} \left[\frac{\partial K}{\partial a_i} - \lambda_j \frac{\partial M}{\partial a_i} \right] \phi_j. \tag{25}$$

While deriving Eq. (25), it is assumed that the eigenvectors have been normalized such that the modal masses are unity. The mode vector derivative may be expressed as a linear combination of all eigenvectors, i.e.

$$\frac{\partial \phi_j}{\partial a_i} = \sum_{q=1}^{d} \beta_{jq} \phi_q, \tag{26}$$

where the coefficients β_{jq} are determined using the generalized eigenvalue problem and orthogonalization properties of eigenvectors. Provided that the eigenvectors have been normalized to unit modal masses, one can get [30]

$$\beta_{jq} = \begin{cases} \phi_q^{\mathrm{T}} \left[\left(\frac{\partial K}{\partial a_i} - \lambda_j \frac{\partial M}{\partial a_i} \right) \Big/ (\lambda_j - \lambda_q) \right] \phi_j, & q \neq j, \\ -\frac{1}{2} \phi_j^{\mathrm{T}} \frac{\partial M}{\partial a_i} \phi_j, & q = j. \end{cases} \tag{27}$$

Because the full eigensystem is not available and far too expensive to solve for, the summation in Eq. (26) is in practice over number $\ll d$ where d is the analytical model order. The value of this number should be high enough in view of condition of gradient matrix.

2.4. Linearization of matrix derivatives

From Eqs. (25) and (27), it can be seen that the derivatives of the structural stiffness and mass matrices, with respect to the design variables, are required. Naturally, the analytical expressions for these entities may be developed, but a new programming effort would be required each time when a new type of design variable is introduced. By adopting the linearized matrix derivatives, viz., first-order Taylor approximation at the current design point, these limitations can be avoided. Hence, it follows that

$$\begin{aligned} \frac{\partial K}{\partial a_i} &= \frac{K(a_i + \Delta a e_i) - K(a_i)}{\Delta a}, \\ \frac{\partial M}{\partial a_i} &= \frac{M(a_i + \Delta a e_i) - M(a_i)}{\Delta a}, \end{aligned} \tag{28}$$

where Δa is the step length and e_i is the vector with ith element equal to 1, and zero elsewhere. It is observed that the expressions are exact in case the matrices are linear with respect to the ith design variable. It should be noted that the evaluation of approximate matrix derivatives according to Eq. (28) does not involve any additional problem solution, but it suffices to assemble and to save the appropriate system matrix for each design variable increment, which is a minor computational effort.

2.5. Optimization algorithm

The optimization algorithm used to minimize the objective function, Eq. (20b), is a standard Trust Region Newton method, which is a sensitivity-based iterative method. Consider the minimization problem

$$\min_{a} \ \Pi(a). \tag{29}$$

The minimization is started at a point a in n-space. To improve the performance it needs to move to a point with a lower function value. The basic idea is to approximate Π with a simpler function q which reasonably reflects the behavior of function Π in a neighborhood N around the point a. This neighborhood is the trust region. A trial step s is computed by minimizing over N. This is the trust region subproblem as follows:

$$\min_{s}[q(s), s \in N]. \tag{30}$$

The current point is updated to be $a+s$ if $\Pi(a+s)<\Pi(a)$, otherwise, the current point remains unchanged and N, the region of trust is shrunk and the trial step computation is repeated. In each iteration p, a quadratic approximation $q(s)$ of $\Pi(a)$ at the current state vector a_p has to be minimized within the trust region Δ_p. In the standard trust-region method [37], the quadratic approximation $q(s)$ is defined by the truncated Taylor series of $\Pi(a)$. The neighborhood N is usually spherical or ellipsoidal in shape. Mathematically, the trust-region subproblem is typically stated by

$$\min_{s} q(s) = \left\{ \frac{1}{2} s^{\mathrm{T}} H_p s + s^{\mathrm{T}} g_p + \Pi_p \text{ such that } \|s\| \leqslant \Delta_p \right\}, \tag{31}$$

where s is a step vector from a_p and H_p, g_p, Π_P are the Hessian (the symmetric matrix of second derivatives), the gradient and the value of the function Π at a_p, respectively. $\|\|$ stands for the 2-norm. After some iterations, the minimum a_* of $\Pi(a)$ is reached where $g(a_*) \approx 0$. The gradient g is obtained from Eq. (21). The Hessian of $\Pi(a)$ is approximated with the gradient information.

3. Case studies

3.1. Simulated simply supported beam

Simulated simply supported beam without damage and with several assumed damage elements are considered. The simulated beam of 6 m length is equally divided into 15 two-dimensional beam elements as shown in Fig. 1. The density and elastic modulus of the material of the beam are 2500 kg/m^3 and 3.2 E+10 N/m^2, respectively. Similarly area of cross section and moment of inertia of simulated beam are 0.05 m^2 and 1.66 E−04 m^4, respectively.

Modal analysis is carried out by developing a program in Matlab environment to get the FE frequencies and mode shapes. All mode shapes have been normalized to the mass matrix. To get the assumed experimental modal parameters, several damages are introduced by reducing the stiffness of assumed elements as shown in Fig. 1. The elastic modulus of elements 3, 8 and 10 are reduced by 20%, 50% and 30%, respectively. The modal analysis is again carried out in this

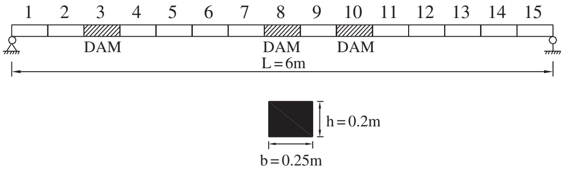

Fig. 1. A simulated simply supported beam.

Table 1
Frequencies and MAC of simulated beam before updating

Mode	Undamaged beam (Hz)	Damaged beam (Hz)	Differences in frequencies (%)	MAC %
1	8.990	8.245	9.035	99.918
2	35.914	34.920	2.846	99.869
3	80.632	75.08	7.394	99.216
4	142.930	137.508	3.943	99.588
5	222.532	209.028	6.460	97.497
6	319.16	313.581	1.779	99.528
7	432.532	405.839	6.577	97.444
8	562.405	547.260	2.767	99.107
9	708.677	671.483	5.539	98.424
10	871.146	836.938	4.087	98.068

damaged beam to get the assumed experimental modal parameters. The initial values of frequencies and corresponding errors and MAC of selected first ten modes are shown in Table 1. The maximum error that appeared in frequency is 9.03% and minimum value of MAC is 97.44%.

The FE model updating procedure explained in theoretical background is implemented in Matlab environment. In this case study, it is assumed that the first 10 bending modes are available and measurements are obtained at all DOFs of the model. Experimental modal flexibility matrix is calculated using the damage induced mode shape and frequency information using Eq. (11). The first ten modes are used to calculate the mode shape sensitivity in Eq. (26). The elastic modulus of each element is used as updating parameters. Thus, there are 15 updating parameters. The tolerances of objective functions and other parameters are set. An iterative procedure for model tuning was then carried out. The pairing of each mode during optimization is ensured with the help of MAC criteria between FE mode shapes and experimental mode shapes.

The selected updating parameters were estimated during an iterative process. After some iteration, the procedure is converged with excellent detection of damaged location and severity. The bar corresponding to no noise case represents the detected damage pattern in Fig. 2. It is clearly seen that the detection of damage on elements 8 and 10 is exact with small error on element 3. There is a negligible error on other elements. The excellent tuning on modal parameters is shown in Table 2.

An important aspect in the development of any model update algorithm is its sensitivity to uncertainty in the measurements. Experimental modal testing is always associated with some kinds of measurement noise or error. This case study presents the results from numerical simulations of noise conducted to study the effects of measurement noise on updating procedure.

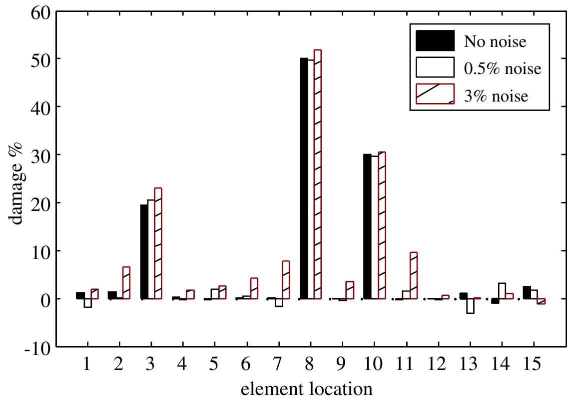

Fig. 2. Location and severity of damage in simulated beam after FE model updating for different cases.

Table 2
Frequencies and MAC of simulated beam after updating

Mode	Before updating (Hz)	Damaged beam (Hz)	After updating (Hz)	Differences in frequencies (%)	MAC %
1	8.990	8.245	8.245	0.007	99.999
2	35.914	34.920	34.916	−0.009	99.999
3	80.632	75.08	75.044	−0.046	99.999
4	142.930	137.508	137.420	−0.063	99.998
5	222.532	209.028	208.884	−0.068	99.997
6	319.16	313.581	313.28	−0.095	99.994
7	432.532	405.839	405.283	−0.136	99.995
8	562.405	547.260	546.611	−0.118	99.992
9	708.677	671.483	670.491	−0.147	99.991
10	871.146	836.938	835.731	−0.144	99.992

To study the effect of measurement noise, it is assumed that the first ten bending modes are available and measurements are obtained at all DOFs of the model. Measurement noise is simulated by adding proportional noise to each of the simulated measured mode shapes. The noise percentage factor remains the same for each mode during a given simulation. The proportional noise is applied to the mode shapes obtained from the simulated damaged beam. Two cases are considered with 0.5% and 3% noise level. The experimental modal flexibility matrix is constructed using Eq. (11) with the noisy mode shapes. Again, the elastic moduli of all 15 beam elements are used as updating parameters.

The similar optimization procedure as explained above is carried out. The damage pattern identified after FE model updating for two noise cases are compared in Fig. 2. In case of 0.5% noise, the damage detection in damaged elements is good with the values of 20.52%, 49.73% and 29.6% in elements 3, 8 and 10, respectively. Some negligible values of damages have appeared on the undamaged elements. When the noise percentage is increased to 3% as, it is observed that the

Table 3
Frequencies and MAC of simulated beam with 3% noise after updating

Mode	Before updating (Hz)	Damaged beam (Hz)	After updating (Hz)	Differences in frequencies (%)	MAC %
1	8.990	8.245	8.085	−1.940	99.993
2	35.914	34.920	34.354	−1.620	99.992
3	80.632	75.08	73.913	−1.554	99.970
4	142.930	137.508	135.333	−1.581	99.923
5	222.532	209.028	205.242	−1.811	99.952
6	319.16	313.581	308.366	−1.663	99.942
7	432.532	405.839	400.675	−1.272	99.963
8	562.405	547.260	537.816	−1.725	99.941
9	708.677	671.483	661.384	−1.503	99.930
10	871.146	836.938	825.920	−1.316	99.851

damaged detection error is increased with values of damage detection 23%, 51.8% and 30.5% on elements 3, 8 and 10, respectively. Also, comparatively more value of damage, for example, 9.6% in element 11, is noticed in undamaged elements also. The tuning on modal parameters in case of 3% noise is shown in Table 3. The table shows that tuning in frequencies and MAC values are good.

This example shows that the noise has an adverse affect on damage detection capability of algorithm. In these simulations, it is assumed that the measurement noise is uniform for all of the measured modes. Actually, the lower experimental modes have less error since the measurement noise is composed of higher-frequency components. As seen from the definition of modal flexibility in Eq. (11), a measured modal flexibility matrix has more contributions from lower modes, the procedure is less affected by the relatively higher errors that appear in high frequency modal measurements.

3.2. Experimental beam

3.2.1. Description of experimental beam and modal parameter identification

The purpose of this experimental study is to identify the damage pattern of the damaged beam using the FE model updating procedure explained in this paper. The cross section of the tested concrete beam of 6 m length is shown in Fig. 3. The reinforcement ratio in a beam is considered to be within a realistic range. By a proper choice of steel quality, the interval between the onset of cracking and beam failure can be made large enough to allow modal analysis at well-separated levels of cracking. To avoid any coupling effect between horizontal and vertical bending modes, the width is chosen to be different from the height of the beam. There are six reinforcement bars of 16 mm diameter, equally distributed over the tension and compression sides, corresponding to reinforcement ratio of 1.4%. Shear reinforcement consists of vertical stirrups of 8 mm diameter at every 200 mm. The total mass of 750 kg results the density of 2500 kg/m^3.

Six-step loaded static tests were conducted to produce the successive damage to the beams. After each static load step, the dynamic measurements were followed up to obtain the dynamic characteristics of damaged beam. In static setup of testing, the beam was loaded by two symmetric point loads at a distance of 2 m as shown in Fig. 3. This test setup produces a central zone of almost uniform damage intensity. At the end of each static load step, before the dynamic test was

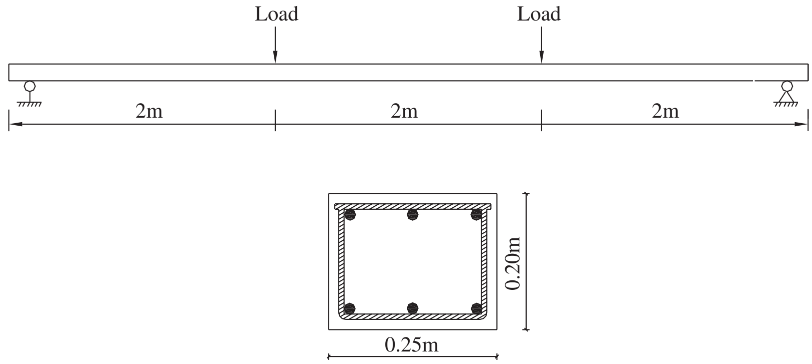

Fig. 3. Static test arrangement and cross section of simply supported beam.

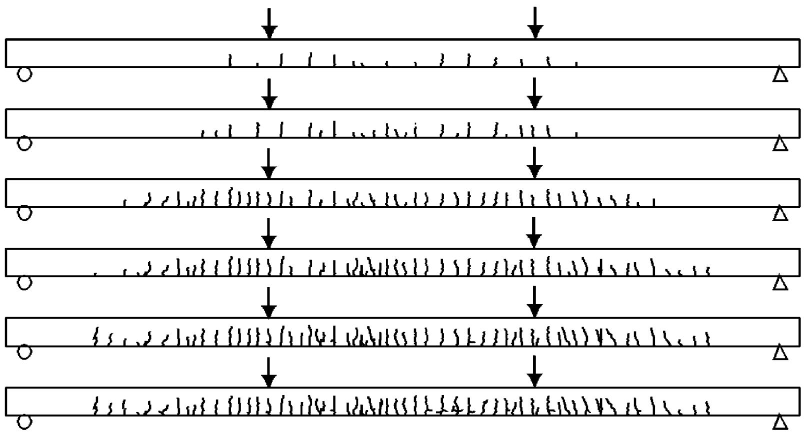
Fig. 4. Observed cracks of the tested beam in each load step.

carried out, the beam surface was visually inspected to locate and quantify the cracks. Fig. 4 shows the observed crack pattern and damage for each static load step. In this study, the load step 5 (24 kN) are aimed to demonstrate the proposed damage identification procedure.

The dynamic testing was carried out on the free–free boundary condition of the beam. The free–free boundary condition avoids the influence of poor defined boundary conditions on the modal parameters. After static load step, the beam was unloaded, the supports were removed and the beam was supported on flexible springs. Acceleration time-histories were vertically measured at every 0.2 m on both sides of the beam with accelerometers. No rotational and longitudinal DOFs were measured. As a result, a total of 62 responses in the vertical direction were recorded in one series. A dynamic force was generated by means of an impulse hammer. But the input was not measured. Dynamic measurement was first performed for the reference (undamaged) state of the test beam. The dynamic characteristics of the reference state serve as an initial value of parameters for current FE model updating.

Before the system identification procedure, the original measurement data often need to be pre-processed. The electrical signals (V) were scaled according to the accelerometer sensitivities to

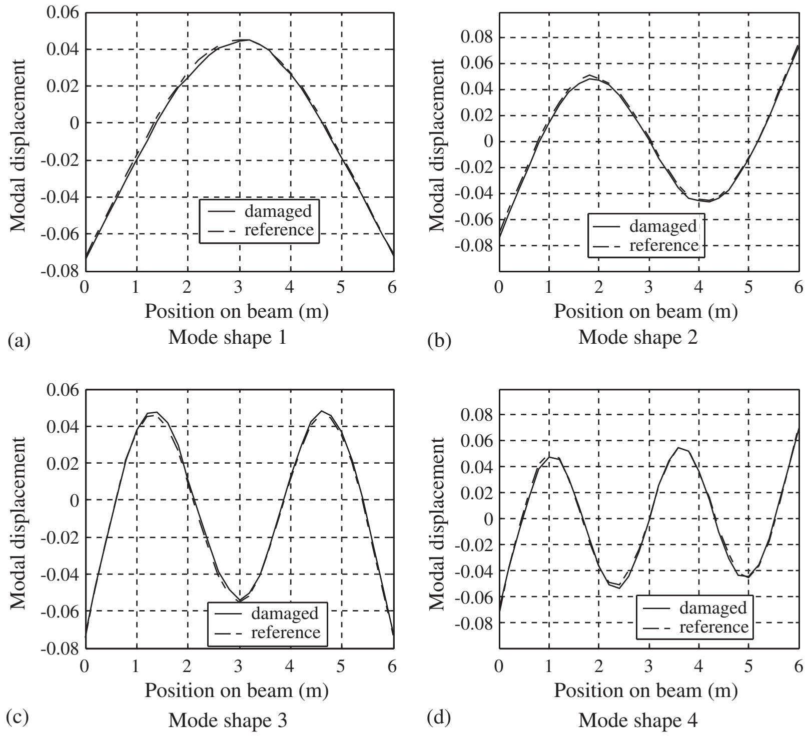

Fig. 5. Identified mode shapes of test beam.

obtain accelerations m/s^2, the DC components were removed, and the data were resampled by a digital low-pass filter. During dynamic testing, the measurement data were sampled at sampling frequency of 5000 Hz. There were 12,288 data points for each channel. The measurement data were resampled at a lower rate of 2500 Hz. This decimation reduces the amount of data without losing information in the frequency band of interest. The stochastic subspace identification, a time-domain technique, is used for system identification. The method is based on the development of a representative linear mathematical model of a dynamic system directly from the observed time series data. The frequencies and mode shape ordinates were identified at both edges of the beam. The average value from two sides was taken to extract the mode shapes of beam, which results 31 measurement points along the length of beam. As explained in theoretical background, the identified first four vertical mode shapes are normalized to initial mass matrix and are shown in Fig. 5.

3.2.2. Model updating and damage detection

The tested beam is analytically modeled with 30 beam elements as shown in Fig. 6. The elastic modulus and inertia moment implemented in the original FE model are 38 GPa and $1.66 \times 10^{-4}\,\mathrm{m}^4$, respectively. The recognized modal parameters for the reference and damage state from system identification and its correlation with initial FE model are shown in Table 4. In the reference state the maximum difference in frequency is 2.18% in the fourth mode and

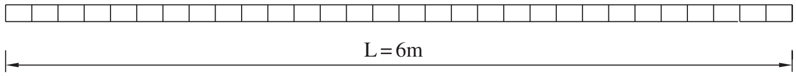

Fig. 6. Descritization of experimental beam.

Table 4
Frequencies and MAC of experimental beam before updating

Mode	Experimental value (Hz)	Initial FE value (Hz)	Differences in frequencies (%)	MAC %
Reference state				
1	21.904	22.213	1.410	99.977
2	60.329	61.065	1.219	99.939
3	117.022	119.287	1.898	99.857
4	192.026	196.320	2.187	99.754
Damaged state				
1	18.005	21.870	21.466	99.881
2	50.204	60.956	21.416	99.850
3	98.219	118.218	20.361	99.796
4	161.876	194.176	19.953	99.345

minimum value of MAC is 99.75% in the same mode. In the damaged case, however, there is a significant difference in the frequencies values in all four modes with maximum difference 21.46% in the first mode. A good correlation in MAC value with minimum of 99.345% in fourth mode is observed.

In carrying out FE model updating, the first 4 bending modes in vertical direction are used in optimization. The experimental modal flexibility matrix is calculated using the experimental mass normalized mode shape and frequency information using Eq. (11). The objective function and gradient are calculated with the help of Eqs. (20a) and (21) respectively. The first 15 FE mode shapes are used to calculate the mode shape sensitivity of Eq. (26). The right pairing of experimental and corresponding analytical mode during iteration are confirmed by using MAC value. The elastic modulus of individual elements is used as updating parameters. As a result, there are 30 updating parameters. Suitable tolerance of objective function and other parameters are set. The selected updating parameters were estimated during an iterative process. The updating is first carried out for the reference state to recognize the damage distribution before static load is applied. After some iteration, the procedure is converged with the detection of damage pattern coefficient a^i defined in Eq. (14a). Fig. 7 shows the stiffness distribution of the beam in reference state after updating. The distribution has random nature with decrease and increase in stiffness along the length. The maximum decrease in stiffness is 10.37% in element 17 and maximum increase in stiffness is 5.92% in element 28. The real pattern of distribution to compare with the updated results is difficult to know. The real pattern depends on the properties of concrete and other uncertainties.

Elastic modulus of each element is corrected using a^i according to Eq. (14b). This corrected value of Elastic modulus is used for the updating of damaged case. The whole optimization procedure is repeated for the damaged case. The detected damage distribution is shown in Fig. 8

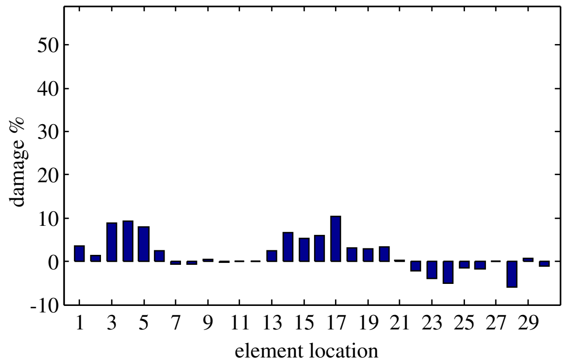

Fig. 7. Location and severity of damage after FE model updating (reference state).

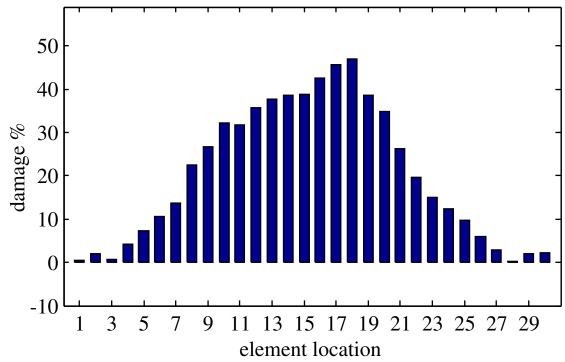

Fig. 8. Location and severity of damage after FE model updating (damaged state).

without the assumed damage pattern [38] or damage function [39]. It is clearly seen that the detected damage is almost symmetrical in nature. The maximum value of damage is within elements 10–20 and the damage goes on decreasing towards both ends of the beam. The damage distribution value of elements 10 and 20 are 32.18% and 34.76%, respectively, with maximum value 46.97% for element 18. Even though the damaged values of elements 10–20 are not perfectly uniform as expected, except elements 16–18 other elements in this range have almost similar values. The obtained values of the frequency and MAC after updating for the reference state and damage state are summarized in Table 5. The comparison of Tables 4 and 5 shows that there is significant improvement in tuning in natural frequencies and also increase in MAC values. In the damaged case, the initial difference of 21.46% in the first mode is decreased to 1.14% after updating. There is also significant improvement in remaining three modes. The maximum difference in frequency is found to be 6.85% in third mode.

The damage detection of the same tested beam was reported in literature [38,39]. It is demonstrated that the identified damage distribution obtained in this paper is comparable with those reported in literatures, despite all the elements in the FE model are used as updating parameters in these case studies which is the extreme adverse condition in FE model updating. Hence, the procedure of FE updating explained in this paper using modal flexibility residual can be successful for the detection of damaged elements.

Table 5
Frequencies and MAC of experimental beam after updating

Mode	Experimental value (Hz)	After updating (Hz)	Differences in frequencies (%)	MAC %
Reference state				
1	21.904	21.870	−0.155	99.982
2	60.329	60.956	1.039	99.940
3	117.022	118.218	1.022	99.861
4	192.026	194.176	1.119	99.768
Damaged state				
1	18.005	17.799	−1.144	99.900
2	50.204	52.676	4.923	99.881
3	98.219	104.951	6.854	99.801
4	161.876	172.429	6.519	99.670

4. Conclusions

A sensitivity-based FE model updating was carried out for damage detection. The objective function consisting of modal flexibility residual was formulated and its gradient was derived. The optimization algorithm used to minimize the objective function and damage detection procedures were presented. The proposed damage detection procedure was illustrated with a simulated example of simply supported concrete beam. The identified damage pattern in this simulated example is excellent. It has been shown that the behavior of the proposed algorithm on noise is satisfactory. The procedure was then verified by the tested reinforced concrete beam, which is damaged in laboratory. Without the assumption of the damaged pattern or damage function of the tested beam, the identified damage distribution was compared with those from the tests and reported in literatures. Despite all the elements in the FE model are used as updating parameters, which is the extreme adverse condition in FE model updating, the damage detection is still acceptable. It is demonstrated that the proposed FE updating using the modal flexibility residual is promising for the detection of damaged elements.

Acknowledgements

Support from the Natural Science Foundation of China (NSFC), under grant number 50378021, is greatly acknowledged.

References

[1] K.D. Hjelmtad, S. Shin, Crack identification in a cantilever beam from modal response, *Journal of Sound and Vibration* 198 (1996) 527–545.
[2] C.P. Fritzen, D. Jennewein, T. Kiefer, Damage detection based on model updating methods, *Mechanical Systems and Signal Processing* 12 (1998) 163–186.
[3] M.S. Agbabian, S.F. Masri, R.K. Miller, T.K. Caughey, System identification approach to detection of structural changes, *Journal of Engineering Mechanics* 117 (1991) 370–390.

[4] H.G. Natke, J.T.P. Yao, *Structural Safety Evaluation Based on System Identification*, Braunschweig/Wiesbaden, Friedr. Vieweg, 1988.
[5] S.W. Doebling, C.R. Farrar, M.B. Prime, D.W. Shevitz, Damage identification and health monitoring of structural and mechanical systems from changes in their vibration characteristics: a literature review, Research Report, LA-13070-MS, ESA-EA, Los Alamos National Laboratory, Los Alamos, N.M., 1996.
[6] P. Cawley, R.D. Adams, The location of defects in structures from measurements of natural frequencies, *Journal of Strain Analysis* 14 (1979) 49–57.
[7] O.S. Salawu, Detection of structural damage through changes in frequency: a review, *Engineering Structures* 19 (1997) 718–723.
[8] A.K. Pandey, M. Biswas, M.M. Samman, Damage detection from changes in curvature mode shapes, *Journal of Sound and Vibration* 145 (1991) 321–332.
[9] P. Cornwell, S.W. Doebling, C.R. Farrar, Application of the strain energy damage detection method to plate like structures, *Proceedings of 15th International Modal Analysis Conference*, Orlando, Florida, 1997, pp. 1312–1318.
[10] A.E. Aktan, K.L. Lee, C. Chuntavan, T. Aksel, Modal testing for structural identification and condition assessment of constructed facilities, *Proceedings of 12th International Modal Analysis Conference*, 1994, pp. 462–468.
[11] A.K. Pandey, M. Biswas, Damage detection in structures using changes in flexibility, *Journal of Sound and Vibration* 169 (1994) 3–17.
[12] G.W. Reich, K.C. Park, Newport Beach California, Experimental application of a structural health monitoring methodology, *Proceedings of the SPIE* 3988 (2000) 143–153.
[13] K. Topole, Damage evaluation via flexibility formulation, smart systems for bridges, structures and highways, *Proceedings of the SPIE* 3043 (1997) 145–154.
[14] J.E. Mottershead, M.I. Friswell, Model updating in structural dynamics: a survery, *Journal of Sound and Vibration* 167 (1993) 347–375.
[15] M.I. Friswell, J.E. Mottershead, *Finite Element Model Updating in Structural Dynamics*, Kluwer Academic Publishers, Dordrecht, 1995.
[16] Maia, Silva, *Theoretical and Experimental Modal Analysis*, Research Studies Press, Baldock, UK, 1997.
[17] M. Link, Updating of analytical models—review of numerical procedures and application aspects, *Proceeding of Structural Dynamics Forum*, Los Alamos, 1999.
[18] A. Berman, E.J. Nagy, Improvements of large analytical model using test data, *AIAA Journal* 21 (1983) 1168–1173.
[19] M. Baruch, I.Y. Bar, Itzhack, Optimal weighted orthogonalization of measured modes, *AIAA Journal* 16 (1978) 346–351.
[20] M. Wang, G. Heo, D. Satpathi, Dynamic characterization of a long span bridge: a finite element based approach, *Soil Dynamics and Earthquake Engineering* 16 (1997) 503–512.
[21] M. Link, R.G. Rohrmann, S. Pietrzko, Experience with automated procedures for adjusting the finite element model of a complex highway bridge to experimental modal data, *Proceedings of 14th International Modal Analysis Conference*, Dearborn, Michigan, 1996.
[22] J.M.W. Brownjohn, P.Q. Xia, H. Hao, Y. Xia, Civil structure condition assessment by FE model updating: methodology and case studies, *Finite Elements in Analysis and Design* 37 (2001) 761–775.
[23] P.W. Moller, O. Friberg, Updating large finite element models in structural dynamics, *AIAA Journal* 36 (1998) 1861–1868.
[24] A. Teughels, J. Maeck, G. De Roeck, A finite element model updating method using experimental modal parameters applied on a railway bridge, *Proceedings of the 7th International Conference on Computer Aided Optimum Design of Structures*, Bologna, Italy, 2001, pp. 97–106.
[25] Q.W. Zhang, C.C. Chang, T.Y.P. Chang, Finite element model updating for structures with parametric constraints, *Earthquake Engineering & Structural Dynamics* 29 (2000) 927–944.
[26] A. Teughels, J. Maeck, G. De Roeck, Damage assessment by FE model updating using damage functions, *Computers and Structures* 80 (2002) 1869–1879.
[27] A. Teughels, Inverse Modelling of Civil Engineering Structures Based on Operational Modal Data, Ph.D. Thesis, Civil Engineering Department, Katholieke Universiteit, Leuven, Belgium, 2003.
[28] S.W. Doebling, Measurement of Structural Flexibility Matrices for Experiments with Incomplete Reciprocity, Ph.D. Thesis, University of Colorado, Department of Aerospace Engineering Sciences, 1995.

[29] A.M. Yan, P. De Boe, J.C. Golinval, Structural damage location by combined analysis of measured flexibility and stiffness, *Progress in Structural Engineering, Mechanics and Computation*, Zingoni, London, 2004, pp. 635–640.
[30] S.W. Doebling, C.R. Farrar, Computation of structural flexibility for bridge health monitoring using ambient modal data, *Proceedings of the 11th ASCE Engineering Mechanics Conference*, 1996, pp. 1114–1117.
[31] A. Hoyos, A.E. Aktan, Regional identification of civil engineered structures based on impact induced transient responses, Research Report 87-1, Louisiana State University, Baton Rouge, 1987.
[32] J. Zhao, J.T. DeWolf, Dynamic monitoring of steel girder highway bridge, *Journal of Bridge Engineering* 7 (6) (2002) 350–356.
[33] E. Parloo, P. Verboven, P. Guillaume, M. Van Overmeire, Sensitivity-based operational mode shape normalization, *Mechanical Systems and Signal Processing* 16 (5) (2002) 757–767.
[34] D. Bernal, B. Gunes, Flexibility based approach for damage characterization: Benchmark application, *Journal of Engineering Mechanics* 130 (1) (2002) 61–70.
[35] MATLAB, *The Language of Technical Computing*, Version 6.1 (Release 12.1), 2001.
[36] R.L. Fox, M.P. Kapoor, Rates of change of eigenvalues and eigenvectors, *AIAA Journal* 16 (1968) 2426–2429.
[37] J.J. More, D.C. Sorensen, Computing a trust region step, *SIAM Journal on Scientific and Statistical Computing* 3 (1983) 553–572.
[38] Wei-Xin Ren, Guido De Roeck, Structural damage identification using modal data. II: test verification, *Journal of Structural Engineering* 128 (2002) 96–104.
[39] J. Maeck, M. Abdel Wahab, G. De Roeck, Damage detection in reinforced concrete structure by dynamic system identification, *Proceedings ISMA 23, Noise and Vibration Engineering*, Leuven, Belgium, 1998, pp. 939–946.